Assessing Accuracy of an Analytical Method *in silico*: Application to "Accurate Constant *via* Transient Incomplete Separation" (ACTIS)

Jean-Luc Rukundo[1], J.C. Yves Le Blanc[2], Sven Kochmann[1], Sergey N. Krylov[1]*

[1]Department of Chemistry and Centre for Research on Biomolecular Interactions, York University, Toronto, Ontario M3J 1P3, Canada
[2]SCIEX, Vaughan, Ontario L4K 4V8, Canada.

Supporting information placeholder

ABSTRACT: Analytical methods may not have reference standards required for testing their accuracy. We postulate that accuracy of an analytical method can be assessed in the absence of reference standards *in silico* if the method is built upon deterministic processes. A deterministic process can be precisely computer-simulated thus allowing virtual experiments with virtual reference standards. Here, we apply this *in silico* approach to study "Accurate Constant *via* Transient Incomplete Separation" (ACTIS), a method for finding the equilibrium dissociation constant (K_d) of protein–small molecule complexes. ACTIS is based on a deterministic process: molecular diffusion of the interacting protein–small molecule pair in a laminar pipe flow. We used COMSOL software to construct a virtual ACTIS setup with a fluidic system mimicking that of a physical ACTIS instrument. Virtual ACTIS experiments performed with virtual samples — mixtures of a protein and a small molecule with defined rate constants and, thus, K_d of their interaction — allowed us to assess ACTIS accuracy by comparing the determined K_d value to the input K_d value. Further, the influence of multiple system parameters on ACTIS accuracy was investigated. Within multi-fold ranges of parameter values, the values of K_d did not deviate from the input K_d values by more than a factor of 1.25 strongly suggesting that ACTIS is intrinsically accurate and that its accuracy is robust. Accordingly, further development of ACTIS can focus on achieving high reproducibility and precision. We foresee that *in silico* accuracy assessment, demonstrated here with ACTIS, will be applicable to other analytical methods built upon deterministic processes.

Accuracy is one of the key performance parameters of quantitative analytical methods. Many methods do not have reference standards and, thus, their accuracy cannot be experimentally tested. We suggest that accuracy of an analytical method can be assessed in the absence of reference standards *in silico* if the underlying physicochemical processes are deterministic, *i.e.* can be precisely simulated. Detailed computer simulation should facilitate virtual experiments in which a virtual sample can be perfectly defined and, thus, can serve as a virtual reference standard. In this work, we applied this *in silico* accuracy assessment to "Accurate Constant *via* Transient Incomplete Separation (ACTIS)".

ACTIS is a separation-based method for finding K_d of complexes (PL) between proteins (P) and small-molecule ligands (L):[1]

$$P + L \underset{k_{off}}{\overset{k_{on}}{\longleftrightarrow}} PL \qquad (1)$$

where K_d is defined *via* equilibrium concentrations of P, L, and PL:

$$K_d = [L]_{eq}[P]_{eq} / [PL]_{eq} \qquad (2)$$

There is no reference standard for the determination of K_d, *i.e.* there is no PL with a known K_d, thus, accuracy of ACTIS cannot be assessed experimentally. On the other hand, ACTIS is built upon a deterministic process of molecular diffusion of P, L, and PL, interacting as in eq 1 while moving within a laminar pipe flow. This process can be precisely described by a set of partial differential equations with precisely defined initial and boundary conditions and precisely defined input values of the rate constants in eq 1: $k_{on,inp}$ and $k_{off,inp}$. The input values of the rate constants define the input value of the equilibrium constants:

$$K_{d,inp} = k_{off,inp}/k_{on,inp} \qquad (3)$$

which can serve as a virtual reference standard in virtual ACTIS experiments. Accordingly, ACTIS is suitable for *in silico* accuracy assessment.

In ACTIS, a short plug of an equilibrium mixture of P and L in a buffer solution is injected into a capillary pre-filled with the pure buffer solution. The plug is then propagated inside the capillary by a pressure-driven flow of the buffer solution.
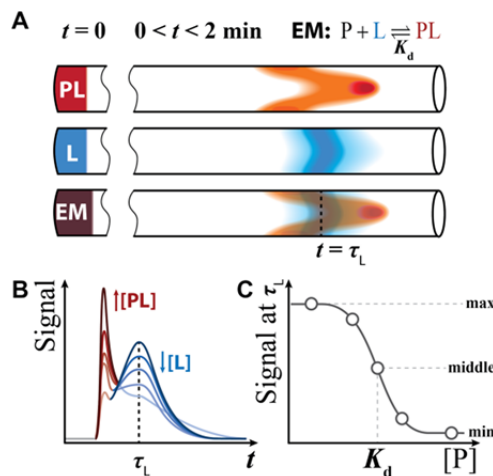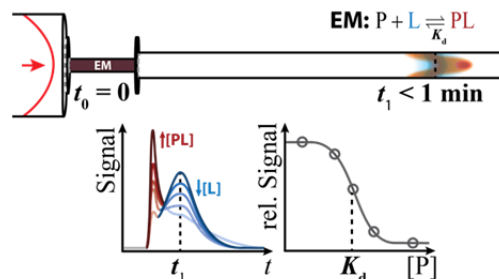

Figure 1. Simplified schematic of determining K_d by ACTIS. **A:** A short plug of the equilibrium mixture (EM) of P and L is propagated through a capillary. Differences in transverse diffusion of PL and L cause their longitudinal separation. **B:** Longitudinal separation results in two peaks, and a cumulative signal from L and PL is measured at time τ_L, which is the characteristic time of transverse diffusion of L. The signal is measured at a constant concentration of L and varying concentrations of P. **C:** A binding isotherm "signal-at-τ_L *vs* concentration of P" is built, and K_d is found as the concentration of P, which corresponds to the signal in the middle between the maximum and minimum signals.

Different rates of transverse diffusion of PL and L in laminar flow cause their transient incomplete separation (TIS) (Figure 1A) resulting in a non-diffusive peak for PL and a diffusive peak for L (Figure 1B). To determine K_d, TIS is performed for a series of equilibrium mixtures with a constant concentration of L and varying concentration of P producing a set of curves termed separagrams (Figure 1B). The cumulative signal of protein-bound L and unbound L is taken at the time corresponding to the maximum of the diffusive peak for each curve. Subsequently, a
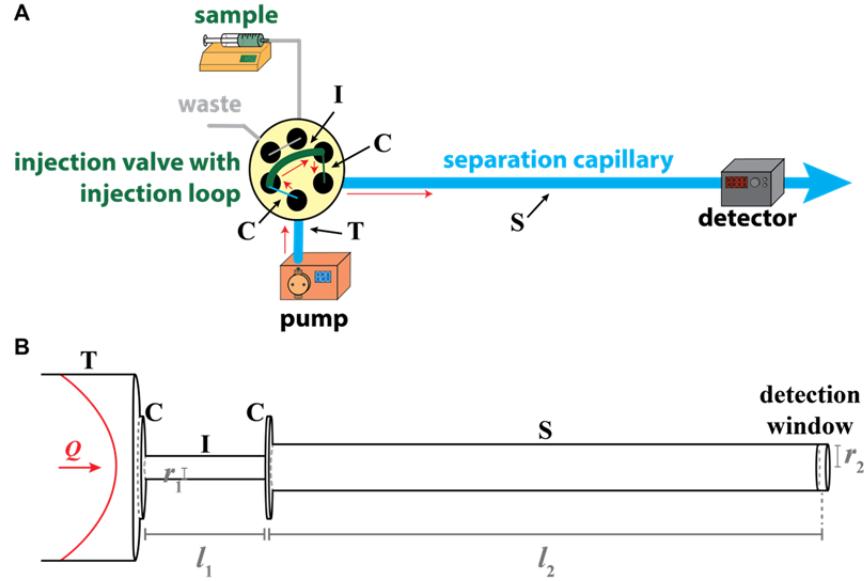
Figure 2. Schematics of a physical (**A**) and computational (**B**) ACTIS instrument. The four letters (**T**, **I**, **S**, and **C**) label the five components simulated in this study and their respective physical counterparts with default dimensions: pump tube (**T**, 5-cm length, 400-μm radius), injection loop (**I**, $l_1 = 13$ cm, $r_1 = 50$ μm), separation capillary (**S**, $l_2 = 50$ cm, $r_2 = 100$ μm) with a detection window (5-mm length, 100-μm radius) at the end, and two identical connectors (**C**, 1.1-mm length, 220-μm radius) linking **T** to **I** and **I** to **S**. Q is the volumetric flow rate provided by a virtual pump. Flow rates were different during sample injection from the loop into the capillary ($Q_{inj} = 5$ μL/min) and during the following TIS stage ($Q_{TIS} = 50$ μL/min). Q_{inj} and Q_{TIS} were not varied in this study. By default, switch between Q_{inj} and Q_{TIS} was set to 10 ms.

classical binding isotherm "signals *vs* concentration of P" is built to reveal the value of K_d (Figure 1C). ACTIS is a uniquely deterministic method as it relies on molecular diffusion in a pressure-driven flow which can be described by a system of partial differential equations with fully-defined initial and boundary conditions.[1–3] As such, it is perfectly suited for computational assessment of its accuracy.

A physical ACTIS instrument has a minimum fluidic system with a pump, an injection loop, a separation capillary, and a multi-port valve (Figure 2A).[1–3] The valve serves as two connectors: one from a pump tube to the injection loop and the other one from the injection loop to the separation capillary. Accordingly, the instrument has five essential fluidic components which can be presented as a series of coaxial pipes of different radii (Figure 2B). We used COMSOL to construct a five-component ACTIS setup depicted in Figure 2B with dimensions identical to those of a physical ACTIS instrument (described in the figure legend). We found that K_d determined in this setup deviated from $K_{d,inp}$, defined by eq 3 and used as a virtual reference standard, by a factor of 1.02. This setup was utilized to study how the accuracy of K_d was affected by variations in: (i) the radius of the injection loop while keeping its volume constant, (ii) the radius of the separation capillary, (iii) shape of the initial (prior to start of TIS) plug of the equilibrium mixture, and (iv) ramp time in flow-rate onset (after the start of TIS). The variations of parameter values used in this study exceeded markedly the ones that are expected in a physical ACTIS setup. We found that despite multi-fold variations in values of a number of parameters, the maximum deviation of K_d from $K_{d,inp}$ was less than a factor of 1.25, suggesting robust intrinsic accuracy of ACTIS.

The intrinsic accuracy of ACTIS has a great practical importance as it allows ACTIS developers to vary instrument configuration without raising concerns about the influence of such variations on accuracy of K_d. Efforts and resources can thus be focused on optimizing instrument configuration to achieve the best reproducibility and the highest precision, the second most important performance parameter of this quantitative analytical method.

■ THEORETICAL BACKGROUND

Here we describe theoretical aspects of ACTIS that are essential for understanding this method at the conceptual level and help establish the theoretical background required for understanding our current work. In particular, we explain basic principles of K_d determination and TIS of L from PL; the corresponding two sections are a close reiteration of our previously published explanation.[1]

General Procedure of K_d Determination. In general, finding K_d requires determination of a fraction R of unbound L in the equilibrium mixture of L and P with the initial concentrations $[L]_0$ and $[P]_0$, respectively:

$$R = [L]_{eq} / [L]_0 \tag{4}$$

Finding R, in turn, requires a signal S that is a superposition of signals from L and PL:

$$S = S_L \times R + S_{PL} \times (1 - R), \quad S_L \neq S_{PL} \tag{5}$$

where S_L and S_{PL} are the signals of pure L ($[L] = [L]_0$, $[PL] = 0$) and pure PL ($[L] = 0$, $[PL] = [L]_0$), respectively; S_L and S_{PL} can be found in experiments with $[P]_0 = 0$ and $[L]_0 \ll [P]_0 \gg K_d$, respectively. The signal from pure P must be negligible with respect to S shown in eq 5 even for $[L]_0 \ll [P]_0 \gg K_d$.

From eq 5, R can be experimentally determined *via* measuring three signals, S_L, S_{PL}, and S, and using the following expression:

$$R_{exp} = (S - S_{PL}) / (S_L - S_{PL}) \tag{6}$$

R can be also expressed theoretically as a function of K_d, $[P]_0$, and $[L]_0$:[1,4]

$$R_{theor} = -\frac{K_d + [P]_0 - [L]_0}{2[L]_0} + \sqrt{\left(\frac{K_d + [P]_0 - [L]_0}{2[L]_0}\right)^2 + \frac{K_d}{[L]_0}} \tag{7}$$

Then, a standard way of finding K_d is to determine R_{exp} for a wide range of $[P]_0$ at a constant $[L]_0$ and to plot a binding isotherm: R_{exp} *vs* $[P]_0$. Finally, this binding isotherm is fitted with eq 7 using K_d

as a fitting parameter and the best fit reveals the sought value of K_d.[1]

Fundamentally, finding R_{exp} with eq 6 requires that S_L and S_{PL} be measurable and that $S_L \neq S_{PL}$. The latter inequality of signals from pure L and pure PL requires that L and PL be "separated" either spectrally or physically.[5] Importantly, complete separation is not required if a signal from the mixture of L and PL is a superposition of signals from individual components L and PL comprising the mixture (see eq 5), and if pure P does not contribute to the cumulative signal from L and PL. As a result, spectral methods that provide only incomplete separation of signals from L and PL (optical spectra of L and LP do overlap typically) are common in finding R_{exp}.[5–7] ACTIS facilitates finding R_{exp} via incomplete physical separation of L and PL.

Transient Incomplete Separation of L from PL. TIS of L from PL will occur always when a short plug of their mixture is propagated within a Hagen-Poiseuille laminar flow in a long capillary. Such a flow is established by a pressure difference between the capillary ends and has a characteristic parabolic profile of flow velocity: the velocity ranges from zero at the capillary walls to its maximum in the capillary center.[8] TIS of L from PL in the longitudinal direction is possible due to the difference in rates of transverse diffusion between small-size L and large-size PL. PL that is near the capillary center will diffuse to the capillary wall slower than L and, thus, will be displaced longitudinally by the flow more than L. PL located near the capillary wall will diffuse to the capillary center slower than L and will be displaced longitudinally by the flow less than L. As a result, during a short transitional stage, a bulk of PL moves faster than a bulk of L, while a tail of PL moves slower than that of L. The separation is incomplete, *i.e.* the longitudinal concentration profiles (concentration *vs* position in the capillary) of L and PL do overlap, even during the transitional stage. Further, this separation gradually dissipates, i.e. the longitudinal concentration profiles of L and PL become symmetrical around the same symmetry axis, after the transitional stage. The after-TIS stage is described by the well-known Taylor dispersion.[9]

Tracking TIS is viewed to be optimal with a flow system in which the optimum distance from the starting position of the equilibrium-mixture plug to the detector (l_{opt}) is linked with the average flow velocity (v_{av}), characteristic time of transverse diffusion of L from the center of the capillary to its inner wall (τ_L), the volumetric flow rate (Q), and diffusion coefficient of L (μ_L), as follows:[1,10]

$$l_{opt} = v_{av}\tau_L = Q / (\pi \mu_L) \qquad (8)$$

where v_{av} relates to Q and the inner capillary radius (r) as:

$$v_{av} = Q / (\pi r^2) \qquad (9)$$

The characteristic time of transverse diffusion across the capillary is defined in general as:

$$\tau = r^2 / \mu \qquad (10)$$

Longitudinal concentration profiles of L and PL are partially separated in the time domain as shown in Figure 1B. Further, if a signal can be measured for each of L and PL, with the above-mentioned detector, inside the capillary or at its exit and is proportional to the average cross-sectional concentration of each of them, $S_L \propto [L]$ and $S_{PL} \propto [PL]$, then, the cumulative signal S satisfies eq 5 and can, thus, be used to determine R_{exp} with eq 6. Finally, R_{exp} can be measured for a wide range of $[P]_0$ to construct a classical binding isotherm R_{exp} *vs* $[P]_0$, which, in turn, can be used to find K_d via fitting the isotherm with eq. 7.

■ DESIGNING A VIRTUAL ACTIS EXPERIMENT

Five-Component Virtual ACTIS Setup. The five-component physical ACTIS system depicted in Figure 2A operates as follows. The injection loop is filled with the sample. The sample is slowly transferred into the separation capillary at a distance equal to the sample-plug length from the capillary entry. The

sample is then propagated fast through the separation capillary to cause TIS of L from PL.

We used COMSOL to construct a virtual five-component ACTIS setup with default dimensions identical to those of a physical ACTIS instrument (Figure 2B). The dimensions of the two connectors are identical and can be considered fixed as well as the dimensions of the pump tube. The dimensions of the injection loop and the separation capillary may need to be changed and, thus, were varied in this study. Of course, the virtual system also contains representations of a virtual pump (a source of a hydrodynamic flow characterized by its volumetric flow rate Q) and a virtual detector (a detection volume inside the capillary), which are also associated with some parameters that can vary and potentially cause inaccuracy in K_d.

A default initial configuration in the virtual five-component setup is the one in which the loop and the loop-capillary connector are filled with the sample, while the remaining components are filled with the buffer solution. This situation mirrors the physical ACTIS setup. In a default virtual ACTIS experiment, the sample is slowly transferred from the injection loop to the separation capillary ($Q = Q_{inj}$) and then propagated fast inside the capillary as in the physical ACTIS experiment ($Q = Q_{TIS}$).

Further in this work, the five-component setup was used first to test the accuracy of K_d for the default geometry (Figure 2B). Then, in a more rigorous study, it was used to investigate how the accuracy of K_d determined with ACTIS was affected by variations in: (i) the radius of the injection loop while keeping its volume constant, (ii) the radius of the separation capillary, (iii) shape of the initial (prior to start of TIS) plug of the equilibrium mixture, and (iv) ramp time in flow-rate onset (after the start of TIS). Below, we provide details on how these four parts of the study were set up.

Geometry of the Injection Loop and Separation Capillary. There are four parameters that characterize the geometry of the injection loop and the separation capillary: the radius (r_1) and length (l_1) of the injection loop and the radius (r_2) of the separation capillary and the distance from the beginning of the separation capillary to the centre of the virtual detector (l_2). We conducted two sets of virtual ACTIS experiments in which r_1 and r_2 were varied. In one set of virtual experiments, r_1 was varied from 5 μm to 5000 μm (l_1 was changed accordingly to keep the volume of the injection loop constant), while r_2 and l_2 were kept constant at default values linked through eqs 8–10. In the other set of virtual experiments, r_2 was varied from 5 μm to 5000 μm while holding constant r_1, l_1, and l_2. The rest of the parameters were default (see Figure 2B).

Geometry of the Initial Sample Plug. While the ideal shape of the initial plug of the equilibrium mixture in the beginning of the separation capillary is cylindrical, in a real experiment, it will be distorted to some degree due to the imperfections of the injection process. To assess how such distortions can affect the accuracy of K_d, we examined square, Gaussian, and half-Gaussian longitudinal distributions of concentrations of L, PL, and P in the initial plug (Figure 3A); cross-sectional concentration profiles were uniform. Here, as opposed to a default way of injecting a 3.0 cm-long sample plug from the injection loop, the same-length initial plug was defined near the entrance of the separation capillary at a distance equal to the plug length, and no injection process was simulated. To model this initial plug shape, the longitudinal (along axis x) distribution of concentrations was defined as a square wave function:

$$f(k_1, k_2, x) = H(k_1 x / L) - H(k_2 x / L - 1) \qquad (11)$$

where $H(kx) = 1/(1 + e^{-2kx})$, which is an analytical sigmoidal approximation of the Heaviside step function.[11] The shape of the plug was varied by varying both k_1 and k_2. The condition of $k_1 = k_2$ corresponds to symmetric plug shapes, *e.g.* for $k_1 = k_2 = 2$ the plug shape is Gaussian and for $k_1 = k_2 = 200$ the plug shape is
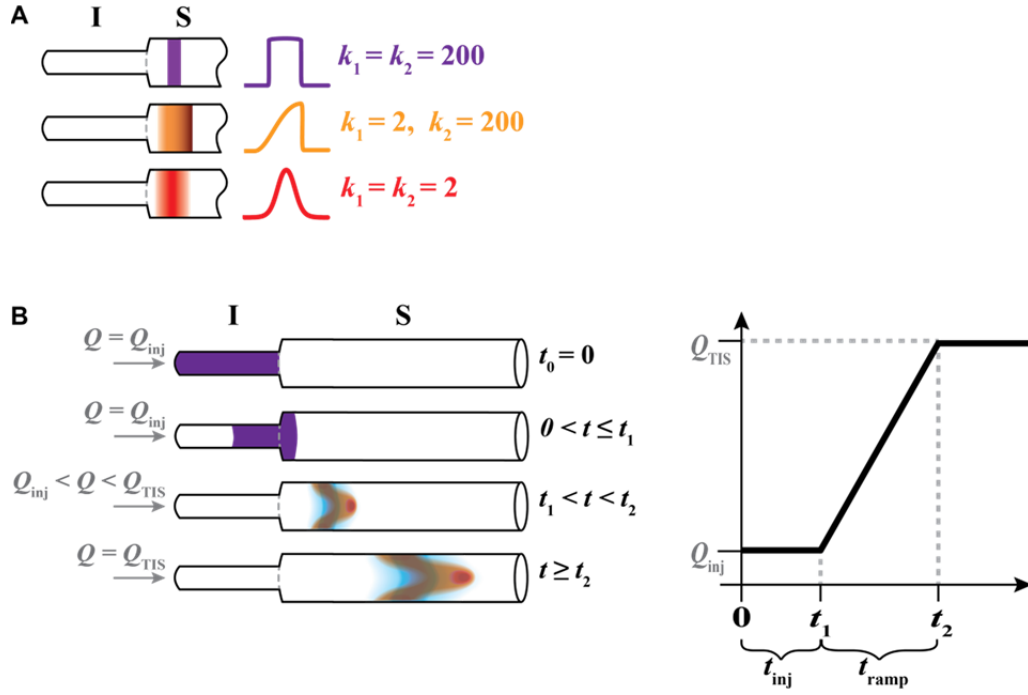
Figure 3. Schematic of the simulated geometries in ACTIS. For clarity the pump tube (T) and connectors (C) are omitted in the presentations here. **A:** A schematic of three different initial plug shapes at the entrance of the separation capillary. Different concentration distributions inside the capillary (left) and longitudinal concentration profiles (result of integration across the capillary, middle) are obtained by changing parameters k_1 and k_2 (right) in the Heaviside function (see text for details). **B:** A schematic showing two key steps in ACTIS: the slow injection of the mixture into the separation capillary and its fast propagation inside the capillary; a transition period required to ramp-up the flow rate connects the two stages. The sample plug is injected from the injection loop into the separation capillary for a time period of t_{inj} at a flow rate of Q_{inj}. Immediately after completing the injection, the volumetric flow rate is set to Q_{TIS} and the plug is further propagated through the separation capillary. The time interval required to reach the propagation flow rate Q_{TIS} is t_{ramp}.

a close approximation of the square function. For $k_1 \neq k_2$ the plug shape is asymmetric, *e.g.* half-Gaussians. The rest of the parameters were default (see Figure 2B).

Ramp Time in Flow-Rate Onset. Achieving and maintaining the ideal plug shape requires the injection of a sample plug from the injection loop into the separation capillary at a slow flow rate of Q_{inj} for a time period of t_{inj}. TIS, on the other hand, requires the propagation of the injected sample plug though the separation capillary at a high flow rate of Q_{TIS}. In a virtual ACTIS experiment, the transition from Q_{inj} to Q_{TIS} can be very fast (e.g. sub-seconds) or even instant. In a real experiment, however, this transition is a process that requires a second-scale time interval of t_{ramp}, *i.e.* the ramp time of the flow rate onset (Figure 3B). In ACTIS, the runtime is relatively short (peaks of PL and L are detected within 30 s), *i.e.* the ramp time of a few seconds may significantly influence TIS of L from PL. Therefore, we varied t_{ramp} to examine the impact of this variation on the profiles of PL and L and, in turn, on the accuracy of K_d determined with ACTIS. The rest of the parameters were default (see Figure 2B).

■ SETTING UP A VIRTUAL ACTIS EXPERIMENT IN COMSOL

To simulate TIS in the five-component setup depicted in Figure 2B we used COMSOL Multiphysics software, version 5.4, with the "Transport of Diluted Species" and "Laminar Flow" modules, which incorporate equations for both mass transfer and reversible binding of P and L in an equilibrium mixture.

Computation time depends on the dimensions of the simulated geometries; thus, to reduce this time, the lengths of all of the five fluidic components can be scaled down along with the length of

the detection window.[1] In such a case, the values of Q_{inj} and Q_{TIS} must also be scaled down to keep the l_2 / Q_{TIS} ratio constant. The scaled down dimensions used in COMSOL computation are reported in SI. Moreover, the mesh size was chosen to minimize computational time and memory requirements. For all the simulations the "*finer mesh*" setting in COMSOL was used with a computational time of ≈ 3 h ($2 \times$ Intel® Xenon® CPU X5690@3.47 GHz, 96 GB RAM); finer settings such as "*extra fine mesh*" resulted in some cases in a better accuracy (up to 10 times better); however, they required an order of magnitude longer computational time (≈ 20 h) (SI).

In all virtual ACTIS experiments, we considered a small-molecule L with typical diffusion coefficient of $\mu_L = 500$ μm^2/s and a large P with a typical diffusion coefficient of $\mu_P = 50$ μm^2/s. The remaining parameters used as COMSOL settings were: $k_{on,inp} = 10^3$ M^{-1}s^{-1}, $k_{off,inp} = 10^{-3}$ s^{-1}, $K_d = k_{off,inp} / k_{on,inp} = 10^{-6}$ M^{-1}, $\mu_{PL} = \mu_P = 50$ μm^2/s, $[L]_0 = 0.5$ μM, $T = 300$ K. $[P]_0$ was varied from 1 nM to 1 mM using 11 different non-zero concentrations plus zero concentration. Three other values of $k_{off,inp}$ *i.e.* 10^{-4}, 10^{-5}, and 10^{-6} s^{-1} with respective values of $K_{d,inp}$, 10^{-7}, 10^{-8}, and 10^{-9} M, were also used in COMSOL. Testing several k_{off} values allowed us to verify the independence of the simulations on a particular value of k_{off}, and, therefore, K_d; the simulations were shown to be consistent with the default value of $k_{off,inp} = 10^{-3}$ s^{-1} (Figure S1).

The sample plug is fully injected during $t_{inj} / 2$ ($t_{inj} = 24$ s). Subsequently, the sample plug is displaced from the entrance of the separation capillary inside the capillary at a distance equal to the plug length during another $t_{inj} / 2$. This displacement is meant to place the initial plug away from the junction between the loop–

capillary connector and the separation capillary; flow disturbance is expected to be the greatest near the junction.

The virtual detector was meant to be at the end of the virtual separation capillary, and virtual detection was performed by averaging concentrations across the capillary within a cylindrical detection window (dimensions: 5 mm × r_2). Experimentally, the cumulative signal S from protein-bound L and unbound L is obtained by averaging points within a time window around the second-peak maximum, *i.e.* the diffusive peak (around time τ_L in Figure 1B).[1] Using a finite-length time window compensates for noise in experimental data; accordingly, we used a finite time window to find the cumulative signal S for all our virtual experiments. Unless otherwise stated, for all the separagrams, the position of the time window was chosen by default by selecting the time at which $S_L > S_{PL}$ and $S_L - S_{PL} = \max$.

All the five fluidic components were modeled as 2D axisymmetric shapes to further reduce computation time in COMSOL.

To study how the variation in the ramp time of flow onset affects the accuracy of K_d, a piecewise function was defined in COMSOL for the linear transition from Q_{inj} to Q_{TIS}, and the length of this transition time, t_{ramp}, was varied.

To study how the variation in plug shape influences the accuracy of K_d, a concentration distribution (eq 11) was defined as an analytical function in COMSOL and, then, varied as explained in the previous section.

Note that neither COMSOL nor any other computational calculation software possesses infinite (numerical) accuracy. COMSOL's inaccuracy will contribute to the assessment of ACTIS's inaccuracy making it an assessment of the *lower limit* of ACTIS accuracy.

■ RESULTS AND DISCUSSION

General Considerations. It is difficult to setup a benchmark for K_d accuracy, but taking into account that variations in K_d determined experimentally often reach orders of magnitude, we consider deviation by less than a factor of 1.25 as acceptable. Accordingly, for the purpose of this work, we consider K_d accurate if $0.80 < K_d / K_{d,inp} < 1.25$. We assume that the virtual ACTIS system is stable (this was confirmed by repeating virtual runs); therefore, we do not provide random errors. Note that we do not consider the detector as a source of imprecision in the following consideration because highly precise detectors for different detection methods, such as fluorescence and mass spectrometry, are available. In fact, any detector that can measure a cumulative cross-sectional average signal from L and PL satisfying eq 5 is suitable for accurate ACTIS measurements provided that it satisfies the following requirements. The detector must have a sufficiently high signal readout speed and a concentration limit of quantitation below K_d values of the studied complexes; the limit of quantification (LOQ = $10 \times S/N$, where N is the level of noise) for L on the used detector should be at least equal to $[L]_0$.[4]

Accuracy of the Default ACTIS Setup. The virtual five-component ACTIS setup, described in the "Setting up a Virtual ACTIS Experiment" section, was first examined for accuracy under default conditions shown in Figure 2B. A full set of separagrams was calculated and K_d was determined from the respective binding isotherm (Figure 4). We found that K_d determined in this setup deviated from $K_{d,inp}$ by a factor of 1.02. The proven accuracy of the default five-component ACTIS setup opened a route for performing a more stringent accuracy test with variations in (i) the radius of the injection loop while keeping its volume constant, (ii) the radius of the separation capillary, (iii) the shape of the initial (prior to start of TIS) plug of the equilibrium mixture, and (iv) ramp time in the flow rate transfer from Q_{inj} to Q_{TIS}.
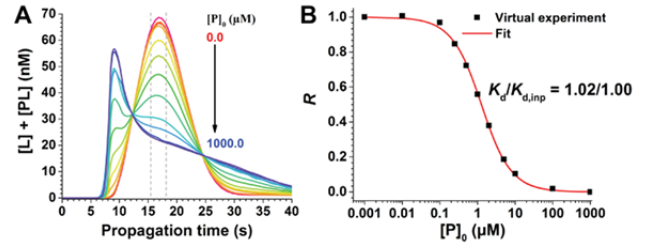

Figure 4. Separagrams (**A**) and a resulting binding isotherm (**B**) for a virtual ACTIS experiment in the five-component fluidic system mimicking a realistic ACTIS setup schematically depicted in **Figure 2**. The dashed lines indicate the time window within which the average signal was taken to calculate the R_{exp} values using eq 6. The binding isotherm was fit with eq 7 with K_d being a fitting parameter.

Variation of Injection-Loop Radius. In this examination, r_1 was varied from 5 to 5000 μm (the default value for r_1 was 50 μm). This variation in r_1 corresponded to variation in r_1/r_2 from 0.05 (= 5/100) to 50 (= 5000/100) for the default value of $r_2 = 100$ μm. To keep the volume of the injection loop constant (which is the purpose of the injection loop), l_1 was changed accordingly for each r_1: $l_1 \sim 1/r_1^2$. The rest of the parameters were default (see Figure 2B).

For each value of r_1, a full set of separagrams has been computed, and the K_d value was determined from a respective binding isotherm (Figure S2). All determined K_d values were compared to $K_{d,inp}$ (Figure 5A). We found that K_d was accurate according to our criteria ($0.8 < K_d / K_{d,inp} < 1.25$) for $r_1/r_2 \le 2.5$ but not for $r_1/r_2 \ge 5$. At $r_1/r_2 = 0.25$ we obtained a binding isotherm with anomalous shape (Figures S2) and $K_d / K_{d,inp} = 1.27$. This anomaly was due to a numerical artifact from meshing in COMSOL; by using a more refined mesh we obtained $K_d / K_{d,inp} < 1.02$. The improvement in accuracy by mesh refinement may suggest that the large deviations in K_d at $r_1/r_2 \ge 5$ are also due to too coarse meshes as well. Thus, more refined and optimized meshes (in particular, for boundary regions between small and large areas) could improve K_d determination in a virtual ACTIS experiment. We confirmed this for the extreme value of $r_1/r_2 = 50$ and found an optimal $K_d / K_{d,inp} = 1.00$ at the expense of excessively increasing the computational time (≈ 72 h instead of ≈ 3 h) and the potential risk of overfitting (SI). In order to keep studies consistent, comparable and in a reasonable time frame as well as to avoid overfitting, we chose the "*finer mesh*" setting from COMSOL without manual optimization for all following studies.

It is instructive to analyze the shapes of the separagrams (Figure S2) to understand the influence of varying r_1 on the TIS process. First, for separagrams at r_1/r_2 of up to 2.5 (= 250/100) they show the two expected peaks — the first for the non-diffusive species (PL) and the second for the diffusive species (L) as in Figure 1B. However, for greater ratios, *i.e.* $r_1/r_2 \ge 5$, the two peaks start merging into one (see shape plots in Figure 5A) followed by a long tail. At these greater ratios, the radius of the injection loop is much larger than that of the separation capillary, and the injection-loop length is very short (Table S1). This large difference between the radii causes the sample plug to take more time to move out of the corner regions of the injection loop that are far removed from the center of the axis (Figure S3) during sample injection. Since the motion of the sample plug out of the injection loop is driven not only by convective motion but also by diffusion, more PL is retained in the injection loop as the sample plug is injected into the separation capillary, since PL diffuses much slowly than L. This retention causes a significant decrease in the signal of PL (Figure S2). In summary, K_d could be accurately determined for ratios $r_1/r_2 \le 2.5$. The ratios $r_1/r_2 \ge 5$ resulted in large deviation in K_d likely due to a combination of
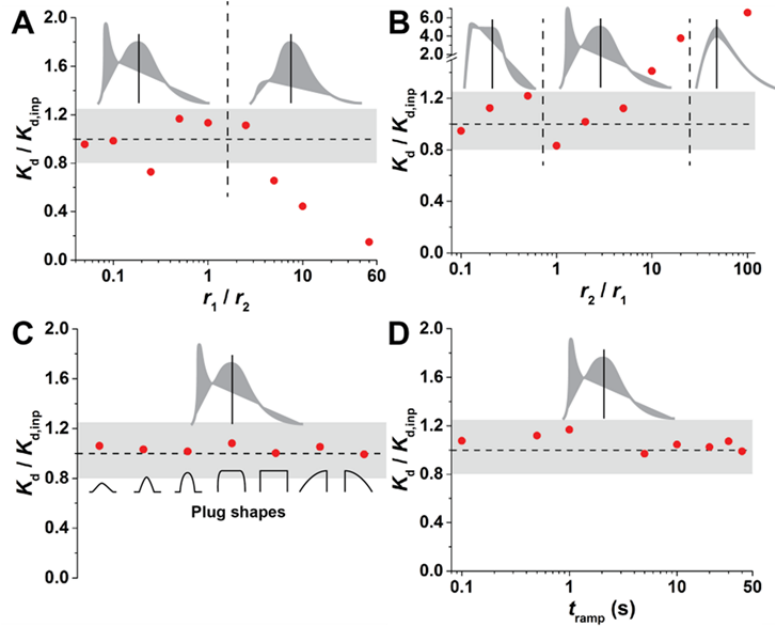
Figure 5. K_d accuracy results of virtual ACTIS experiments by varying: **A**: injection loop radius (r_1), **B**: separation capillary radius (r_2), **C**: injection plug shape, and **D**: propagation pump ramp time (t_{ramp}). The red dots mark the evaluated relative K_d values. The grey area in each panel marks the range in $K_d / K_{d,inp}$ (from 0.8 to 1.25) which is considered as the "area of accuracy" in this study; the horizontal black dashed line marks the target relative K_d value (1.0). The small separagram figures in each panel show the change of separagram shape when varying the abscissa parameter; the vertical black line indicates the position of the detection window at which the evaluation was done; shaded areas show the magnitude of change in the ordinate when varying $[P]_0$. See the text and supporting information for more details.

mesh size limitations and non-optimal TIS conditions; however, it is to be noted that these ratios correspond to $r_1 > 500$ μm and $l_1 < 500$ μm which are impractical parameters for a physical ACTIS instrument.

Variation in Separation-Capillary Radius. In this examination, the value of r_2 was varied from 5 to 5000 μm. Thus, the ratio r_2 / r_1 (note the ratio is *opposite* to r_1 / r_2 from the previous study) varied from 0.1 (= 5/50) to 100 (= 5000/50) for a fixed value of $r_1 = 50$ μm. The rest of parameters were default (Figure 2B). Note that while the ratios between r_1 and r_2 change in this and the previous examinations, these two sets of virtual experiments are not identical as decreasing r_2 while keeping r_1, l_1, and l_2 constant lead to situations when the plug length is comparable to the length of the separation capillary, which is a greatly suboptimum condition.

For each ratio r_2 / r_1, a full set of separagrams has been calculated, and the K_d value was determined from a respective binding isotherm (Figure S4). All determined K_d values were compared to $K_{d,inp}$ (Figure 5B). K_d values were accurate according to our criteria ($0.8 < K_d / K_{d,inp} < 1.25$) for $r_2 / r_1 \leq 5$ (= 250/50). For $r_2 / r_1 > 5$, the deviation of K_d from $K_{d,inp}$ was beyond the acceptable range; specifically, in this case the values of K_d were overestimated: $K_d / K_{d,inp} > 1.4$.

Again, it is instructive to analyze the shapes of the separagrams (Figure S4). They show two classical peaks corresponding to the non-diffusive species (PL) and diffusive species (L) (as in Figure 1B) for r_2 / r_1 between 1 (= 50/50) and 20 (= 1000/50). For $r_2 / r_1 < 1$, however, the non-diffusive peak becomes less pronounced (see the left shape plot in Figure 5B), which can be attributed to the plug-length ($l_{plug} \geq 52$ cm) being greater than the distance from the capillary inlet to the detection window $l_2 = 50$ cm). Consequently, most of PL and L in the equilibrium mixture cannot be separated before they reach the detector. Obviously, reducing the plug length by adjusting the injection loop would solve this issue and return these cases to the optimum conditions. Still, K_d deviated from the input $K_{d,inp}$ by less

than a factor of 1.25 implying that K_d could be accurately determined from these curves.

For $r_2 / r_1 > 5$, both peaks merged into a single diffusive one (see the right shape plot in Figure 5B). Here, the time of separation (≥ 500 s) is comparable with or greater than the characteristic time of complex dissociation ($\approx 1 / k_{off} = 1000$ s); therefore, the injected sample plug is no longer in the state of equilibrium. Moreover, the transfer flow between the small-radius injection loop and the large-radius separation capillary results in the phenomenon of "flow separation".[12] In this situation, the flow lines are no longer parallel across the whole cross section of the separation capillary. Indeed, recirculation of the flow occurs near the capillary walls (Figure S5) leading to remixing, which affects TIS of L from PL. Additionally, the Péclet number Pe for large r_2 (> 500 μm) becomes smaller than 40 and suggesting that longitudinal diffusion along the separation capillary becomes non-negligible at $r_2 / r_1 > 5$ ($Pe \approx 42$, Table S1 and S2).[13] All the above non-optimal conditions, *i.e.* the departure from equilibrium, the "flow separation" phenomenon, and significant longitudinal diffusion, likely contribute to the large deviation in K_d from $K_{d,inp}$ at $r_2 / r_1 > 5$.

In summary, K_d could be accurately determined for $r_1 / r_2 \leq 5$. The ratios $r_1 / r_2 \geq 10$ resulted in large deviation in K_d due to the different non-optimal conditions described previously and likely due to sub-optimal meshing. However, if one works within the range of optimal conditions, which correspond to $r_1 / r_2 \leq 5$ in our case, it can be concluded that the accuracy of K_d determination by ACTIS is invariant with respect to changes in the separation capillary radius.

Variation in the Shape of the Initial Plug. For this study, the plug shape was varied ranging from an ideal cylindrical shape to conical shapes and to asymmetrical shapes. Here, as opposed to injecting the plug from the injection loop, the initial plug was defined at the entrance of the separation capillary; no injection process with Q_{inj} was simulated; only the TIS-causing propagation at Q_{TIS} was computed. The variation in concentration distributions

in the initial plug was done by changing parameters k_1 and k_2 of the Heaviside function as illustrated in Figure 3A. The rest of the parameters were default (see Figure 2B). For each plug shape, a full set of separagrams has been calculated, and a K_d value was determined from a respective binding isotherm (Figure S6). All determined K_d values were compared to $K_{d,inp}$ (Figure 5C).

For all examined plug shapes, K_d could be accurately determined, *i.e.* $0.99 \leq K_d / K_{d,inp} \leq 1.08$. The shapes of the separagrams show the two peaks corresponding to the non-diffusive species (PL) and diffusive species (L) (as in Figure 1B) for all plug shapes. All separagrams were only minimally affected by the variations in the plug shape demonstrating that ACTIS was robust towards large variations in the plug shape and proving that moderate imperfections in plug shape expected in real experiments would not affect the accuracy of K_d measurements.

Variation in Ramp Time of Flow Onset. The ramp time t_{ramp} was varied from 0.10 to 40 s as illustrated in Figure 2C. The total run time was 60 s with the diffusive peak (L) arriving to the detector between 15 and 30 s. The rest of the parameters were default (see Figure 2B). For each value of t_{ramp}, a full set of separagrams has been obtained, and a K_d value was determined from a respective binding isotherm (Figure S7). All determined K_d values were compared to $K_{d,inp}$ (Figure 5D). For all examined t_{ramp}, K_d could be accurately determined, *i.e.* $0.97 \leq K_d / K_{d,inp} \leq 1.17$. The shapes of the separagrams show the two peaks corresponding to the non-diffusive species (PL) and diffusive species (L) (as in Figure 1B) for all t_{ramp}. Overall, separagram shapes change only slightly; only positions of the non-diffusive and diffusive peaks move from 10 to 25 s and from 17 to 35 s, respectively (Figure S7). These results show that accuracy of K_d determination with ACTIS is robust towards changes in ramp time of the flow onset.

■ CONCLUSION

In this work, we examined and proved the robustness of ACTIS, in a virtual fluidic system resembling the one of a real ACTIS instrument, towards large variations in the parameters characterizing both the fluidic system and the flow. We used COMSOL to construct a virtual five-component ACTIS setup exactly mimicking the geometry of a physical assembly (Figure 2). K_d determined in this setup deviated from $K_{d,inp}$, by a factor of only 1.02.

This five-component ACTIS setup was also used to study how accuracy of K_d is affected by variations in: (i) the radius of the injection loop while keeping its volume constant, (ii) the radius of the separation capillary, (iii) shape of the initial (prior to start of TIS) plug of the equilibrium mixture, and (iv) ramp time in flow-rate onset (after the start of TIS). The variations used in the test exceeded markedly the ones that could be caused by undesirable variations expected in a physical ACTIS setup. The tested variations provide wide ranges for desirable experimental instrumental adjustments which would not make ACTIS inaccurate. In general, the values of K_d did not deviate from the input K_d values by more than a factor of 1.25 upon variations in the above parameters.

Regarding the variation of the injection loop radius, we found that K_d could be accurately determined for $0.05 \leq r_1 / r_2 \leq 2.5$. Larger ratios, *i.e.* $r_1 / r_2 \geq 5$, corresponding to injection loop radii much greater than the separation capillary radius resulted in deviations greater than by a factor of 1.25 likely due to a combination of mesh-size limitations and non-optimal TIS conditions.

Accuracy of K_d was also not affected greatly by variation of the separation capillary radius if $r_2 / r_1 < 10$. Note that for $r_2 / r_1 \leq 0.5$ the signal variation in the separagram becomes much smaller caused by the plug length being comparable to the separation capillary length (Table S2). A small signal variation

will make it difficult to evaluate separagrams containing noise, *e.g.* from experimental data. Great deviations in K_d were observed for $r_2 / r_1 \geq 10$ due the departure from equilibrium of the injected sample plug, the "flow separation" phenomenon, and significant longitudinal diffusion, with deviation in K_d of $K_d / K_{d,inp} > 1.25$. The mesh-size limitations likely also contribute to the observed deviations.

Moreover, deviations in plug shape from the ideal cylindrical shape do not influence the accuracy of K_d. If plug injection is reproducible from run to run, the determined K_d will be accurate.

Finally, large variations in the pump ramp time for flow onset do not influence the accuracy in K_d, *i.e.* cost-effective pumps with slow ramp times can be used for ACTIS.

From the above results and our experience, we recommend the following strategy to setup an ACTIS instrument. First, one should choose the propagation flow rate (Q_{TIS}) as well as the separation capillary dimensions (r_2 and l_2) so that the ligand L reaches the detector at time τ_L (see eqs. 8–10) which is much shorter than anticipated lifetime of the complex ($1 / k_{off}$). Our choice of $\tau_L \approx 10$ s should suffice most of the stable PL complexes. Second, the injection loop radius r_1 should be selected to be 0.5–1.0 times the separation capillary radius r_2. For instance, a separation capillary radius of 100 μm corresponds to a range in injection loop radius of 50–100 μm. Third, the ACTIS instrument should be assembled using the straightforward scheme provided in Figure 2; an elaborate setup proposed in our preliminary study[1] is not needed since parameters such as the plug shape or ramp time have only minimal impact on K_d accuracy according to the results of our current study.

Our findings and recommendations will allow ACTIS-instrumentation developers to change (simplify) instrument configuration drastically without raising questions about how such changes may affect accuracy of K_d. By relying on ACTIS intrinsic accuracy, developers can focus their efforts and resources on optimizing instrument configuration to achieve the highest precision. Finally, to the best of our knowledge, this work provides the first example of a comprehensive proof of accuracy of an analytical method performed in-silico. We foresee that the in-silico accuracy-assessment approach will be used for a similar task on other methods built upon processes with the deterministic nature.

■ ASSOCIATED CONTENT

Supporting Information
The Supporting Information is available free of charge on the ACS Publications website and on ChemRxiv (**DOI:** 10.26434/chemrxiv.12345644).

Theoretical background for computer simulation and data evaluation; Simulation of separagrams; Figure S1, Variation in $k_{off,inp}$ − separagrams and binding isotherms; Figure S2, Variation in injection loop dimensions – separagrams and binding isotherms; Figure S3, Variation in injection loop dimensions – sample-plug distribution; Figure S4, Variation in separation capillary radii – separagrams and binding isotherms; Figure S5, Velocity streamlines at different separation capillary radii; Figure S6, Variation in the initial plug shape – separagrams and binding isotherms; Figure S7, Variation in ramp time of flow onset – separagrams and binding isotherms; Table S1+S2, Péclet number and plug length
(PDF)
Evaluation files with raw data (ZIP)
Model files of Numerical simulations in COMSOL (ZIP)

■ AUTHOR INFORMATION

Corresponding Author

*E-mail: skrylov@yorku.ca.

ORCID

Sergey N. Krylov: 0000-0003-3270-2130
J.C. Yves LeBlanc: 0000-0002-3801-3590
Jean-Luc Rukundo: 0000-0003-3626-2515
Sven Kochmann: 0000-0001-7423-4609

Author Contributions

The manuscript was written through contributions of all authors, and all authors have given approval to the final version of the manuscript before the submission.

Notes

The authors declare no competing financial interest.

■ REFERENCES

(1) Sisavath, N.; Rukundo, J.-L.; Le Blanc, J. C. Y.; Galievsky, V. A.; Bao, J.; Kochmann, S.; Stasheuski, A. S.; Krylov, S. N. Transient Incomplete Separation Facilitates Finding Accurate Equilibrium Dissociation Constant of Protein–Small Molecule Complex. *Angew. Chem. Int. Ed.* **2019**, *58*, 6635−6639.

(2) Harada, M.; Kido, T.; Masudo, T.; Okada, T. Solute Distribution Coupled with Laminar Flow in Wide-Bore Capillaries: What Can Be Separated without Chemical or Physical Fields? *Anal. Sci.* **2005**, *21*, 491−496.

(3) Okada, T.; Harada, M.; Kido, T. Resolution of Small Molecules by Passage through an Open Capillary. *Anal. Chem.* **2005**, *77*, 6041−6046.

(4) Kanoatov, M.; Galievsky, V. A.; Krylova, S. M.; Cherney, L. T.; Jankowski, H. K.; Krylov, S. N. Using Nonequilibrium Capillary Electrophoresis of Equilibrium Mixtures (NECEEM) for Simultaneous Determination of Concentration and Equilibrium Constant. *Anal. Chem.* **2015**, *87*, 3099−3106.

(5) Pollard, T. D. A Guide to Simple and Informative Binding Assays. *Mol. Biol. Cell* **2010**, *21*, 4057−4298.

(6) Jameson, D. M.; Ross, J. A. Fluorescence Polarization/Anisotropy in Diagnostics and Imaging. *Chem. Rev.* **2010**, *110*, 2685−2708.

(7) Wu, P.; Brand, L. Resonance energy transfer: methods and applications. *Anal. Biochem.* **1994**, *218*, 1−13.

(8) Umehara, R.; Harada, M.; Okada, T. Wide-bore hydrodynamic chromatography in sub-second range. *J. Sep. Sci.* **2009**, *32*, 472−478.

(9) Taylor, G. I. Dispersion of soluble matter in solvent flowing slowly through a tube. *Proc. R. Soc. A: Math. Phys. Eng. Sci.* **1953**, *219*, 186−203.

(10) Umehara, R.; Miyahara, H.; Okino, A.; Harada, M.; Okada, T. Wide-Bore Capillary Hydrodynamic Chromatography with ICP-MS Detection for Evaluation of Lanthanide Uptake by Molecular Aggregates. *Anal. Sci.* **2012**, *28*, 359−365.

(11) Kythe, P. K. *Sinusoids: Theory and Technological Applications* **2014**, Chapman and Hall/CRC.

(12) Durst, F. *Fluid Mechanics. An Introduction to the Theory of Fluid Flows* **2007**, Springer.

(13) Chamieh, J.; Leclercq, L.; Martin, M.; Slaoui, S.; Jensen, H., Østergaard, J.; Cottet, H. Limits in Size of Taylor Dispersion Analysis: Representation of the Different Hydrodynamic Regimes and Application to the Size-Characterization of Cubosomes. *Anal. Chem.* **2017**, *89*, 13487−13493.